

Breathers and Photoinduced Absorption in Polyacetylene

A. R. Bishop, D. K. Campbell, and P. S. Lomdahl
*Center for Nonlinear Studies and Theoretical Division, Los Alamos National Laboratory,
 Los Alamos, New Mexico 87545*

and

B. Horovitz^(a)
Department of Nuclear Physics, The Weizmann Institute of Science, Rehovot, Israel

and

S. R. Phillpot
*Physics Department, University of Florida, Gainesville, Florida 32611
 (Received 27 September 1983)*

The dynamics of *trans*-polyacetylene is studied within the adiabatic model of Su, Schrieffer, and Heeger. A single soliton has a maximum velocity, v_m , which can be higher than the sound velocity. A long-time simulation shows that, from an initial electron-hole pair, a soliton and antisoliton emerge with velocities $\pm v_m$ and that a persistent breather is left behind. This breather may account for the high-energy intragap structure observed in photoinduced absorption, including isotope dependence.

PACS numbers: 71.38.+i, 72.15.Nj, 72.80.Le

Charged kink solitons (S) can be generated in *trans*-(CH)_x either by doping or by photoexcitation. Dynamical studies^{1,2} of the SSH model³ have shown that a photogenerated electron-hole pair evolves into a charged soliton-antisoliton ($S\bar{S}$) pair. Photoinduced absorption experiments have indeed shown features similar to those seen in the absorption of doped samples.⁴⁻⁸ A "mid-gap" absorption at ~ 0.5 eV appears, similar to the doping-induced absorption at $\sim 0.6-0.7$ eV. Three infrared lines appear in both cases; the shifts in their frequencies are well accounted for by a change of a single pinning parameter.⁹ In photoinduced absorption, however, there is an additional peak at ~ 1.35 eV,^{4,6} which is absent in doping experiments. This feature has previously been associated⁴ with a 1A_g excited state, which in finite polyenes is found,¹⁰ as a consequence of Coulomb interactions, to lie below the optical gap. Here we show that there is another mechanism which may explain this absorption feature: namely, the *nonlinear dynamics* of the coupled electron-phonon system.

We begin by studying a single moving soliton and showing, first by an analytic estimate and then with quantitative numerical calculations, that it has a maximum velocity, v_m , of propagation. To develop the analytic estimate consider a uniformly moving soliton with the traveling wave form¹¹ $\Delta(x) = \Delta_0 \tanh[(x - vt)/\xi(v)]$, where $2\Delta_0$ is the optical gap ($\cong 1.5 - 1.6$ eV). With this *Ansatz* and in the adiabatic limit ($\omega_0 \ll \Delta_0$, ω_0 being the bare phonon frequency), we find that $\xi(v)$ is deter-

mined by minimizing the action

$$A = \Delta_0 \{ 2/\pi + (1 - 2/\pi)(1 - x)^2 - \alpha/x \}, \quad (1)$$

where $x = \xi/\xi_0$, $\xi_0 \equiv \xi(0)$, $\alpha \equiv 2v^2\Delta_0^2/3\pi\lambda v_F^2\omega_0^2$. Here v_F is the Fermi velocity, and λ the dimensionless electron-phonon coupling constant [$\cong 0.2$ in *trans*-(CH)_x].^{3,11} The first term in Eq. (1) is the soliton rest energy, the second is an approximation (roughly valid¹¹ in the region $0 < x < 1$) to the excess energy due to the velocity-dependent shape deformation, and the final term is the kinetic energy.¹¹ Equation (1) has extrema only when $\alpha < \alpha_c \cong 0.11$; at this critical value, $x_c = \frac{2}{3}$. α_c provides an immediate upper limit on the soliton velocity of $v_m = (6\pi\alpha_c\lambda)^{1/2}v_s\xi_0/a = 1.4\lambda^{1/2}v_s\xi_0/a$, which corresponds to a kinetic energy of $\sim 0.1\Delta_0$. (a is the lattice constant and $v_s = \omega_0 a/2$.) Since the hyperbolic tangent form is a restricted *Ansatz*, there may be an instability at a lower velocity. The width ξ , however, would still stay close to ξ_0 . Now if $\xi(v)/v < \omega_R^{-1}$, with $\omega_R = \omega_0(2\lambda)^{1/2}$ the renormalized phonon frequency, then the ions cannot respond to the reversal of the dimerization pattern caused by the soliton's motion. This defines a similar maximum velocity $v_m \cong \omega_R \xi(v_m) \cong \lambda^{1/2}v_s\xi_0/a$. Since for (CH)_x $\xi_0 \cong 7a$,³ with $\lambda \cong 0.2$ we have $v_m \cong 4v_s$; thus the maximum soliton velocity is greater than the sound velocity.

To test this analytic estimate we have numerically integrated the SSH equations of motion^{1,3} and have indeed found a critical velocity (see Fig. 1). For $\xi_0 = 7a$, we find $v_m \cong 2.7v_s$, while for a system with $\xi_0 = 2.75a$, we obtain $v_m \cong 0.6v_s$. In-

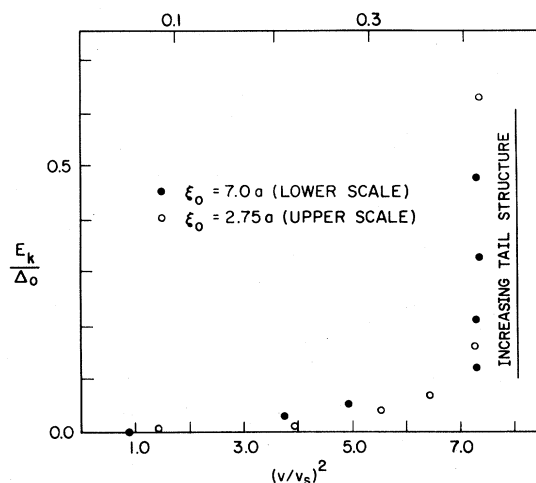


FIG. 1. Kinetic energy E_k of a moving soliton from simulations as a function of $(v/v_s)^2$, where v is the average velocity and $v_s = \frac{1}{2}\omega_0 a$ is the sound velocity. For $E_k \geq 0.1\Delta_0$ uniform soliton propagation is not observed; an oscillatory tail develops. Parameters are (notations of Refs. 1 and 2), for solid circles, $\alpha = 4.1$ eV/Å, $t_0 = 2.5$ eV, $K = 21$ eV/Å², $\omega_0 = 2.48 \times 10^{14}$ sec⁻¹; and for open circles, $\alpha = 4.8$ eV/Å, $t_0 = 2.5$ eV, $K = 17.3$ eV/Å², and $\omega_0 = 2.25 \times 10^{14}$ sec⁻¹.

dependent of other parameters, we also find a critical kinetic energy, $E_k \approx 0.1\Delta_0$, above which uniform soliton translation is not observed and an oscillating tail structure develops. With regard to the supersonic propagation of solitons, we recall that our dynamical simulation is adiabatic^{1,2} and ignores quantum phonon emission which leads to soliton damping.¹² However, the lifetime due to this effect is long¹² ($\approx 10^{-7}$ sec) on the scale of the picosecond photoabsorption phenomena we now discuss.

Consider the photoexcitation of an electron from the top of the valence band to the bottom of the conduction band;^{1,2} the energy input is $2\Delta_0$. As shown previously,^{1,2} this initial electron-hole pair quickly develops into a separating pair of charged¹³ solitons. Our long-time simulations show that the separating solitons move with $v \approx v_m$ and only modest shape distortion. Therefore, their total kinetic energy is close to $0.2\Delta_0$. Hence the sum of their rest energy ($\approx 4\Delta_0/\pi \approx 1.3\Delta_0$)^{3,11} and kinetic energy ($\geq 0.2\Delta_0$) is $\geq 1.5\Delta_0$; the excess energy of $\approx 0.5\Delta_0$ is concentrated in a well-localized, oscillatory "breather" excitation, left behind by the separating solitons. The breather is charge neutral and hence, like the ground state,⁹ should not be strongly sensitive to Coulomb correlations.

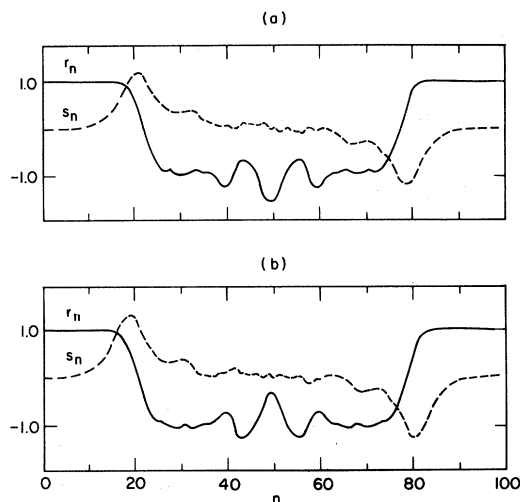


FIG. 2. Dimerization pattern r_n relative to the local lattice constant (full line); the slope of s_n is the change in the lattice constant (dashed line). Both r_n and s_n are in units of the ground-state dimerization $u_0 \approx 0.10a$. Parameters correspond to the second set of Fig. 1. (a) Time = 279 (in units of 10^{-15} sec) after photogeneration; (b) time = 299. The time difference of 20 units is 0.54 phonon periods or 0.51 breather periods.

In Fig. 2 we present the results of a dynamical simulation on a 98-atom chain with periodic boundary conditions and $\xi_0 = 2.75a$. The coupling of the moving solitons to the acoustic phonons results in a local contraction of the lattice constant around the solitons' centers. The actual ion displacement at site n is of the form $u_n = (-1)^n \bar{u}_n + n\delta a$, where δa is the change in the lattice constant and the (slowly varying) \bar{u}_n represents the dimerization pattern relative to the local lattice constant. Hence in Fig. 2 we plot $r_n \equiv \frac{1}{4}(-1)^n [2u_n - u_{n+1} - u_{n-1}]$ and $s_n \equiv \frac{1}{4}[2u_n + u_{n+1} + u_{n-1}]$, so that $r_n \approx \bar{u}_n$ and $s_n \approx n\delta a$. As anticipated, the results for s_n indeed indicate that both S and \bar{S} locally contract the lattice constant. More striking is the clear existence of a separate, well-localized breather excitation; its oscillatory behavior in time is indicated by the two parts of Fig. 2, which show two times separated by $\sim \frac{1}{2}$ the observed breather period. To check the persistence of this breather we have isolated the central 42 atoms and followed their dynamics up to 5 ps ($= 5000$ time steps of the computer code ≈ 130 phonon periods). On this time scale, the breather persists with no appreciable reduction in amplitude.¹⁴

Figure 3 shows the time dependence of the electronic levels. The mid-gap states associated

with the separating solitons quickly settle to zero [Fig. 3(a)]. The next electronic state is also split significantly from the continuum states and exhibits large-scale oscillations [Fig. 3(b)]. This state (and its symmetric counterpart above mid-gap) is associated with the localized breather. From fits to the numerical data its frequency is $\approx 0.95\omega_R$ and its average position is shifted from Δ_0 to $\sim 0.8\Delta_0$. Repulsion from the continuum levels results in the asymmetric form of Fig. 3(b).

An important support for these numerical results is the following analytic solution for small-amplitude breathers in the continuum limit. We start from the effective Lagrangian for $\Delta(x, t)$, which to lowest order in derivatives is¹⁵ (the phase variable is fixed at zero in the present model¹¹)

$$\mathcal{L} = \frac{2}{\pi v_F} \left\{ \frac{1}{2} \Delta^2 \left(\ln \frac{2E_c}{\Delta} + \frac{1}{2} \right) - \frac{\Delta^2}{4\lambda} - \frac{v_F^2 \Delta'^2}{24\Delta^2} + \frac{\dot{\Delta}^2}{4\lambda\omega_0^2} \right\}, \quad (2)$$

where E_c is the electronic cutoff energy and $\Delta_0 = 2E_c \exp(-1/2\lambda)$. Using multiple-scale asymptotic perturbation theory or following the strategy previously applied to the φ^4 theory,^{14,16} we expand $\Delta(x, t) = \Delta_0(1 + \delta(x, t))$ and find

$$\delta(x, t) = 6^{1/2} \epsilon \operatorname{sech}[(12)^{1/2} \epsilon x / \xi_0] \cos[(1 - \frac{1}{2}\epsilon^2)\omega_R t] + \frac{3}{2} \epsilon^2 \operatorname{sech}^2[(12)^{1/2} \epsilon x / \xi_0] \left\{ \frac{1}{3} \cos[2(1 - \frac{1}{2}\epsilon^2)\omega_R t] - 1 \right\} + O(\epsilon^4), \quad (3)$$

where ϵ is the small expansion parameter, $\xi_0 = v_F / \Delta_0$, and $\omega_R = \omega_0(2\lambda)^{1/2}$. The time-independent term represents a local decrease in the gap. The breather energy is $E_B = \Delta_0 [2\sqrt{3}/\pi] \epsilon [1 - 5\epsilon^2/9 + O(\epsilon^4)]$. The breather can be semiclassically quantized¹⁷ by the condition¹⁶ $\int dx dt (\dot{\Delta}^2 / \omega_R^2) = 2n\pi$, where the time integral is over one period, giving

$$E_B = n\omega_R [1 - (\pi^2/72)(\omega_R^2 / \Delta_0^2)n^2 + O(n^4)]. \quad (4)$$

Testing the consistency of (3) with the classical energy expression on the breather shown in Fig. 2, we estimate that $\epsilon = 0.32$ and, therefore that $E_B \approx 0.33\Delta_0$ and the time-averaged local gap is shifted from Δ_0 to $0.85\Delta_0$, in fair agreement with the numerical data. Given this consistency and that the important energies scale *only* with Δ_0 (e.g., critical kinetic and breather energies), we can directly apply our results with parameters appropriate to $(\text{CH})_x$.

We next show that our results can explain several properties of the photoinduced absorption data which have yet to be explained by the approach based on Coulomb correlations.^{4,10} The classical breather has two electronic states in-

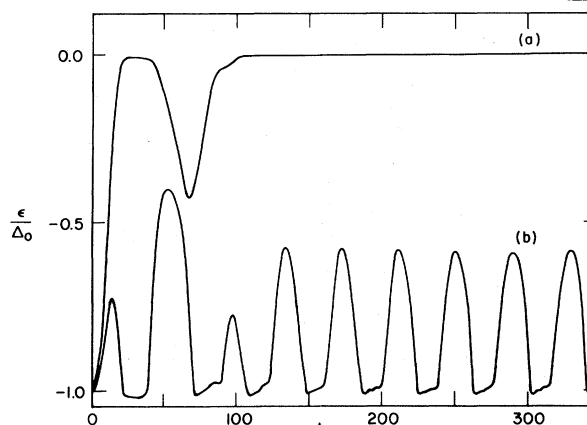


FIG. 3. Time dependence of electronic levels: (a) state at top of valence band, rapidly becoming a mid-gap state; (b) next state in valence band, shifting into the gap and oscillating with breather frequency. Parameters are those of Fig. 2.

side the normal gap, the lower one doubly occupied and the upper one empty. Thus the main experimental signature of the breather is that its optical absorption contains a line *below* the continuum band edge at $2\Delta_0$. The presence of the photoinduced absorption at 1.35 eV^{4,6} is thus consistent with our simulations, which show simultaneously photogenerated charged solitons and a breather. For $\epsilon = 0.32$ the inferred normal gap is ≈ 1.6 eV, consistent with other estimates. It is important to note that the induced absorption of both the 1.35-eV peak and the mid-gap saturate at the same input power.¹⁸ This indicates that both phenomena are generated simultaneously, as we predict.

The breather in *trans*-(CH)_x can decay to the ground state by phonon emission, since no electronic transitions are needed. Thus the absorption line we attribute to the breather should decay faster than the infrared and mid-gap absorptions associated with the charged solitons. This difference in decay times should be enhanced as the temperature increases, as is observed experimentally.^{4,6}

In *cis*-(CH)_x a photoinduced line is also observed below the band edge.⁴ But here the absence of ground-state degeneracy leads to confinement of the electron-hole pair to a localized exciton, which our dynamical simulations show oscillates in time qualitatively like the breather in *trans*-(CH)_x. One important difference, however, is in the occupation of electronic levels; the decay of the *cis*-(CH)_x exciton involves an electronic transition. Hence we expect this decay to be much less sensitive to increased temperature, which is also consistent with the data.⁴

Finally, a direct manifestation of the nonlinear ion dynamics would be an isotope dependence of the 1.35-eV line in *trans*-(CH)_x and the structure below the gap. Under the assumption that breathers with the same quantum number are generated in both (CH)_x and (CD)_x, those in (CD)_x should, from Eq. (4), have lower energies. Recent experimental data¹⁹ show such an isotope dependence, demonstrating directly that the nonlinear ion dynamics considered here is essential for understanding this phenomenon.

We are grateful to J. Orenstein and Z. Vardeny for detailed discussions of their published and unpublished data, and to J. R. Schrieffer, E. J. Mele, and T. D. Schultz for helpful comments. Two of us (B.H. and S.R.P.) thank the Center for Nonlinear Studies, Los Alamos National Laboratory, for hospitality. This research was supported by grants from the Los Alamos Computing Division, the U. S. Department of Energy, and the U. S.-Israel Binational Science Foundation, Jerusalem, Israel.

(a)Present address: Physics Department, Ben-Gurion University, Beer Sheva, Israel.

¹W. P. Su and J. R. Schrieffer, Proc. Natl. Acad. Sci. U.S.A. **77**, 5626 (1980).

²E. J. Mele, Phys. Rev. B **26**, 6901 (1982).

³W. P. Su, J. R. Schrieffer, and A. J. Heeger, Phys. Rev. Lett. **42**, 1698 (1979), and Phys. Rev. B **22**, 2099 (1980) (referred to here as the SSH model).

⁴J. Orenstein and G. L. Baker, Phys. Rev. Lett. **49**, 1043 (1982).

⁵Z. Vardeny, J. Strait, D. Moses, T. C. Chung, and A. J. Heeger, Phys. Rev. Lett. **49**, 1657 (1982).

⁶C. V. Shank, R. Yen, A. L. Fork, J. Orenstein, and G. L. Baker, Phys. Rev. Lett. **49**, 1660 (1982).

⁷G. B. Blanchet, C. R. Fincher, T. C. Chung, and A. J. Heeger, Phys. Rev. Lett. **50**, 1938 (1983).

⁸Z. Vardeny, J. Orenstein, and G. L. Baker, Phys. Rev. Lett. **50**, 2032 (1983).

⁹Z. Vardeny, E. Ehrenfreund, O. Brafman, and B. Horovitz, Phys. Rev. Lett. **51**, 2326 (1983).

¹⁰For a review, see B. Hudson, B. E. Kohler, and K. Schulten, in *Excited States*, edited by C. C. Lim (Academic, New York, 1982), Vol. 6, p. 1.

¹¹H. Takayama, Y. R. Lin-Liu, and K. Maki, Phys. Rev. B **21**, 2388 (1980); B. Horovitz, Phys. Rev. B **22**, 1101 (1980).

¹²K. Maki, Phys. Rev. B **26**, 2187 (1982).

¹³R. Ball, W. P. Su, and J. R. Schrieffer, J. Phys. (Paris), Colloq. **44**, C3-429 (1983).

¹⁴Concerning the very long-time stability of these breathers, it is useful to recall results on similar breatherlike states found in the ϕ^4 model. In low-velocity kink-antikink collisions in ϕ^4 , the kinks are trapped into a breatherlike state which, although gradually reducing in amplitude, remains clearly identifiable for more than 500 periods [C. A. Wingate, SIAM (Soc. Ind. Appl. Math.) J. Appl. Math. **43**, 120 (1983)]. The problem of the existence of "exact" ϕ^4 breathers has been studied numerically (D. K. Campbell and J. W. Negele, unpublished) and the results support their existence. Likewise, molecular-dynamics simulations (T. R. Koehler, unpublished) show persistent breathers at finite temperatures.

¹⁵B. Horovitz and J. A. Krumhansl, Solid State Commun. **26**, 81 (1978), and Phys. Rev. B, to be published.

¹⁶R. F. Dashen, B. Hasslacher, and A. Neveu, Phys. Rev. D **11**, 3424 (1975).

¹⁷Our quantization approach here differs from a standard quantum chemical technique only in the order of calculation, which is more practicable for systems with large numbers of degrees of freedom. Comparative studies are in progress.

¹⁸J. Orenstein, private communications.

¹⁹Z. Vardeny and J. Tanaka, to be published.